**American Journal of Biological and Environmental Statistics**
2021; 7(1): 1-8
http://www.sciencepublishinggroup.com/j/ajbes
doi: 10.11648/j.ajbes.20210701.11
ISSN: 2471-9765 (Print); ISSN: 2471-979X (Online)

**Review Ariticle**

# Perovskite Based Photocatalyst for Wastewater Treatment: Green Approach of Environmental Sustainability

**Ajit Das[1], Dipankar Mahata[2], Mrinal Kanti Adak[3, *]**

[1]Department of Chemistry, Balarampur College, Balarampur, West Bengal, India

[2]Department of Environmental Science/Studies, Balarampur College, Balarampur, West Bengal, India

[3]Department of Chemical Sciences, Indian Institute of Science Education and Research Mohali, Punjab, India

## Email address:

bubunkumaradak@gmail.com (M. K. Adak)

[*]Corresponding author

## To cite this article:

Ajit Das, Dipankar Mahata, Mrinal Kanti Adak. Perovskite Based Photocatalyst for Wastewater Treatment: Green Approach of Environmental Sustainability. *American Journal of Biological and Environmental Statistics*. Vol. 7, No. 1, 2021, pp. 1-8. doi: 10.11648/j.ajbes.20210701.11

**Received**: January 24, 2021; **Accepted**: February 1, 2021; **Published**: February 9, 2021

**Abstract:** Persistent organic substances in wastewater are creating serious problems to the living world as well as to the environment, thereby creating huge detrimental impact on the ecosystem. In view of the grave situation, removal of the persistent organic substances from wastewater effluent holds a great promise to balance the ecosystem and to sustain societal impact value. In this respect, perovskite based photocatalysts have achieved remarkable attention to the scientific community due to their unique structural features and flexibility of composition. Again, surface polarization and electric dipole-dipole interaction in the perovskite material make them attractive for photocatalytic application. This review paper summarized the photocatalytic activity of perovskite materials and their modification to enhance catalytic activity for wastewater treatment. The modification in perovskite has been done to reduce bandgap energy for enhanced visible light activity, separation of charge carriers for their long lifetime, and fast photocatalytic reaction. The recent investigation of $ABO_3$ type perovskite, layered perovskite, and halide type of perovskite photocatalysts have been discussed detailly. The modification of corresponding perovskites by doped and formation of heterojunction is investigated carefully. The formation and identification of reactive oxygen species (ROS) and their degradation mechanism by trapping experiment and ESR technique has been summarized here. Finally, large scale with energy and environmental related research should be processed for a permanent solution of wastewater problem.

**Keywords:** Perovskite, Photocatalyst, Wastewater Treatmenr, Reactive Oxygen Species

## 1. Introduction

Water pollution and its proper treatment show a huge impact point in current time due to rapid growing population, urbanization, and industrial development [1]. Pollutants in water cause serious hazards to the ecosystem and also create severe health issues for humans like respiratory problems, asthma, dermatitis, mutagenicity, cancer, etc [2]. Renewable green energy is considered for future sustainability of human civilization due to limited non-renewable sources of fossil fuel and its polluted nature. In this respect, solar energy is much attractive due to easy handling, free availability, and cleanliness [3, 4]. Solar energy based photocatalysis systems show much affectivity for the treatment of wastewater without generation of secondary pollutants. Photocatalysis is a rapidly growing field for potential application with clean environmental nature [5]. In the photocatalytic system, the advanced oxidation process (AOP) is much more effective through the production of ROS [6]. Highly active ROS species lead to the degradation and mineralization of pollutant compounds in wastewater [1, 7].

In the photocatalytic application, perovskite materials show much interest due to their common availability as oxide, narrow band gap, wide wavelength for solar light absorption, structural flexibility and high power conversion efficiency [8–11]. The above characteristics lead perovskite material to high density research for wastewater treatment. $ABO_3$ is the general formula of perovskite oxide structure, where 'A' is

alkali metal or alkaline earth metal or rare earth metal and 'B' is usually transition metal. In the structural feature of perovskite, 'A' atom reside at the corner of the lattice with 12 oxygen atoms coordination and 'B' atom reside at center position with 6 oxygen atoms coordination [12, 13]. The main problem of a perovskite material is the large bandgap that only prefers UV light absorption. A good photocatalyst should have absorbance near 520 nm as the major portion of solar light consists of visible and NIR region [14]. The photocatalytic activity of perovskite material may be tuned in different ways of design due to their chemical stability and band structure characteristics [13, 15, 16]. The band gap of perovskite can be modified by the replacement of 'A' or 'B' or 'O' atoms or introduction of different kind atoms [14, 17].

In this review article, recent reports of perovskite photocatalytic materials are summarized on basis of their organic pollutant removal capability. Modified and unmodified $ABO_3$ type perovskite, layered perovskite, and halide perovskite photocatalytic materials are discussed according to their photocatalytic efficiency. The degradation mechanism and role of reactive oxygen species to identify the degradation path is also reviewed here.

## 2. Photocatalytic Pathway

In a photocatalytic process, a photocatalyst uses photon as a source of energy to enhance chemical reaction rate without being involved in the reaction. $TiO_2$ was discovered as a photocatalyst in 1972 during water splitting in a photo-electrochemical reaction [18]. Under light irradiation on a photocatalyst, the electrons absorb energy from the valence band (VB) and excited to the conduction band (CB). The excitation of electrons from VB to CB creates a hole ($h^+$) at the conduction band. The capability of a photocalyst depends on the excitement of the electron, separation of the electron and hole, and photo-oxidation reduction reaction at the catalyst surface [19]. In such reactions, the light energy should be greater than the bandgap energy of the material ($h\upsilon \geq E_g$, where $h\upsilon$ is the light energy and $E_g$ is the bandgap energy).

$$Photocatalyst + h\upsilon \rightarrow photogeneratedcharges\ (e^- and h^+)$$

The photogenerated holes is then react with water and form hydroxyl radical ($^{\bullet}OH$) at the surface of the material. $^{\bullet}OH$ is a powerful oxidizing agent and attacks organic molecules non-selectively and mineralizes them according to their structure and stability. Photoexcited electron in the conduction band reacts with oxygen to form superoxide anion radical ($^{\bullet}O_2^-$) and take part in the oxidation process of organic molecules. The $^{\bullet}O_2^-$ also react with proton to form hydroperoxyl radical ($^{\bullet}OOH$), which is responsible for the formation of hydrogen peroxide ($H_2O_2$). Dissociation of $H_2O_2$ again generates highly reactive $^{\bullet}OH$ [20].

$$H_2O + h^+ \rightarrow HO^{\bullet} + H^+$$

$$O_2 + e^- \rightarrow O_2^{\bullet -}$$

$$O_2^{\bullet -} + H^+ \rightleftarrows HOO^{\bullet}$$

$$2HOO^{\bullet} \rightarrow H_2O_2 + O_2$$

$$H_2O_2 \rightarrow 2HO^{\bullet}$$

$$Dye + HO^{\bullet} \rightarrow CO_2 + H_2O$$

$$Dye + h^+(VB) \rightarrow Oxidation\ products$$

$$Dye + e^-(CB) \rightarrow Reduction\ products$$

The degradation mechanism is schematically given in Figure 1. The accurate assessments of an active photocatalyst can be measured through apparent quantum efficiency (AQE) [14].

$$AQE = \frac{numberofreactedelectrons}{numberofincidentphotons} \times 100\%$$

In $ABO_3$ type perovskite, the 2p orbitals of oxygen atoms are responsible for the formation of lower energy level valence band and 3d orbitals of 'B' atoms constitute the conduction band [13].

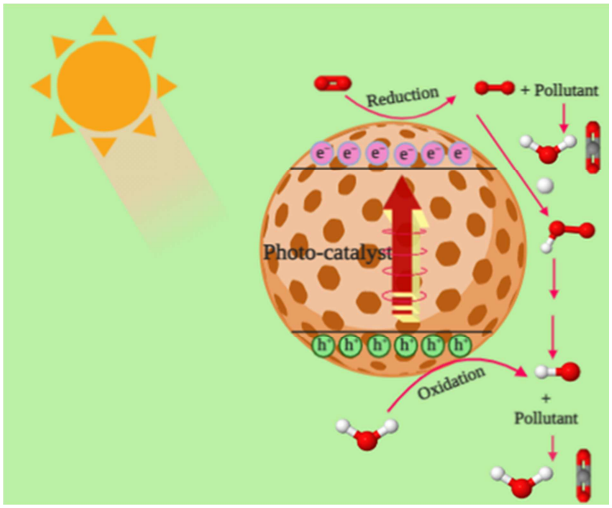


***Figure 1.*** *Schematic representation for the photocatalytic degradation of organic pollutant.*

## 3. Importance of Perovskite Photocatalyst

### *3.1. $ABO_3$ Type Perovskites*

Visible light driven $LaNiO_3$ is modified with $TiO_2$ to form heterojunction composite catalysts that exhibit superior photocatalytic efficiency for the degradation of methyl orange (MO) and ciprofloxacin. The combination of n-type $TiO_2$ and p-type $LaNiO_3$ form S-scheme heterojunction that shorten the electron transfer route from inner to surface [13]. Hexahydroxy-stannates ($MSn(OH)_6$ (M=Cu, Zn)) show photocatalytic properties for the degradation of methylene blue (MB). In this perovskite material, the 'A' site induces

lattice distortion through $d^{10}$-$d^{10}$ configuration though the ionic radius of Cu, Zn is almost the same. In the degradation mechanism, scavengers study shows that photo-generated holes play a dominant role for MB degradation, where superoxide and hydroxyl radicals take an assistant role [21]. Visible light active $BaBiO_3$ shows good photocatalytic activity for the decomposition of rhodamine B (RhB) and water splitting. $BaBiO_3$ that annealed at 800°C showed higher catalytic study than low temperature hydrothermal synthesized material due to higher crystallinity, smaller particle size, lower recombination rate of charge carriers, and lower resistance [22]. Green capping agent, corn assisted $LaFeO_3$ perovskite nanostructured show high catalytic efficiency for the degradation of organic pollutant erythrosine and eriochrome black T. Under UV light irradiation, the photocatalyst degrade 96% erythrosine and 84% eriochrome black T in 90 min [23]. Lanthanum and Chromium codoped $SrTiO_3$ ($SrTiO_3$(La, Cr)) has removed 83% tetracycline in 90 min under photocatalytic reaction. In the degradation mechanism, the presence of $Cr^{3+}$ enhances the formation of superoxide radical, which is the main active species [24]. Gong *et al*. have been used $LaFeO_3$ to decorate $TiO_2$ nanotube arrays through an electrochemical method to enhance quantum efficiency under sunlight irradiation. Involvement of this p-type third generation perovskite photocatalyst enhances charge carrier lifetime and their separation efficiency through the improvement of photocatalytic activity. The formation of heterojunction between $LaFeO_3$ and $TiO_2$ leads to Fermi energy level apt to align in equilibrium and built-in an electric field at the interface of heterojunction. In the degradation mechanism, under visible light irradiation, the photogenerated electrons are transferred from the CB of $LaFeO_3$ to the CB of $TiO_2$ that reduces the recombination rate of charge carriers [17]. 3.2 at.% Ti substitution in $LaFeO_3$ leads to the 100% total organic carbon (TOC) removal from the 4-chloro phenol aqueous solution under UV-A light irradiation [25]. Undoped and Gadolinium-doped $MTiO_3$ perovskites (M=Co, Cu, and Ni) show photocatalytic activity for the degradation of MB dye under visible light irradiation. $CoTiO_3$, $CuTiO_3$ and $NiTiO_3$ degrade 31.42%, 61.12% and 30.10% MB within 120 min whereas, this degradation efficiency increase to 43.64%, 74.19%, and 88.64% by doping 2% of Gd in the perovskite material respectively. The enhancement of degradation efficiency is due to the reduction of electron hole recombination rate by the introduction of Gd. The presence of partially filled 4f orbital of Gd facilitates to trap conduction band electron and leads to the formation of superoxide anion radical according to the following way [26]:

$$Gd^{3+} + e^{-} \rightarrow Gd^{2+}(electron\ trapping\ step)$$

$$Gd^{2+} + O_2(ads) \rightarrow Gd^{3+} + O_2^{\bullet -}(ads)\ (electron\ transferring\ step)$$

Subramanian *et al*. have been synthesized $BiFeO_3$-$Bi_2S_3$, $BiFeO_3$-$NiS_2$, and $BiFeO_3$-$NaNbO_3$ heterostructured visible light active photocatalyst for the degradation of organic pollutants. Among the heterostructured, $BiFeO_3$-$Bi_2S_3$ show reduced band gap energy (1.4) and able to degrade 97% MB upto 3 cycle [27]. Microwave-ultraviolet (MW-UV) double response active Z-scheme $SrTiO_3/MnFe_2O_4$ photocatalyst successfully degrades tetracycline as a target pollutant. In the Z-scheme system, n-type semiconductor $SrTiO_3$ (Eg=3.40 eV) has used photosystem-I where $MnFe_2O_4$ (Eg=1.74 eV) has used photosystem-II. The combined 300W microwave and 200W ultraviolet system is eligible to completely degrade tetracycline pollutants within 20 min in pseudo first order pathway [28]. Mn- and Ce- codoped $BaTiO_3$ [29] show photocatalytic activity for the degradation of congo red and titan yellow dye solution as shown in Figure 2.

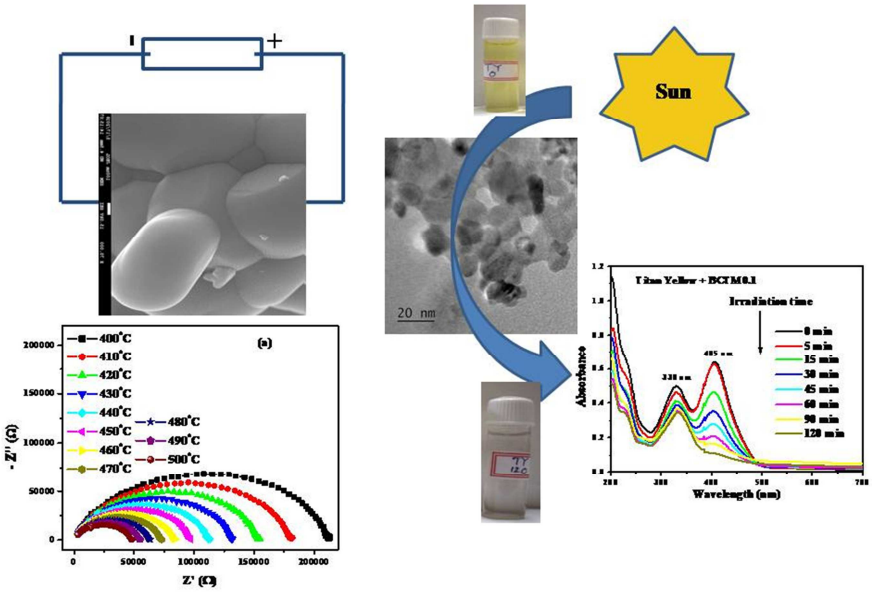


***Figure 2.*** *Schematic diagram for the photocatalytically degradation of titan yellow by -Mn and -Ce doped $BaTiO_3$ (reprinted with permission from ref [29]. Copyright © 2020, Elsevier).*

### *3.2. Layered Structured Perovskites*

In layered perovskite structure, the network arrangement of octahedrons has boosted the mobility charge carriers with high quantum yield efficiency [30]. Hua *et al*. have been synthesized N-doped $La_2Ti_2O_7$ decorated on graphene sheets through the attachment of Ti-N bond, Ti-C bond, and oxynitrides. The composite material shows high photocatalytic activity for the decomposition of bisphenol A under visible light irradiation and degrades 81% within 300 minute. The mixing of N 2p states and O 2p states extend optical adsorption characteristics of the composite. Again, the presence of graphene enhances the ability for the charge separation and transformation that enhance catalytic activity [30]. Heterojunction formation by the combination of oxygen vacant bismuth tungstate nanosheets (BWO-OV) and oxygen-enriched graphitic carbon nitride (OCN) show high photocatalytic efficiency for tetracycline degradation. This 3D Z-scheme heterojunction built an electric field that accelerates the interfacial charge transfer. Under light irradiation, electrons are excited from Bi 4p orbital to Bi 6p orbital and form an electric field that reduce recombination rate of charge carriers [31]. $Bi_2WO_6$ has been grown vertically on $Ta_3N_5$ nanofibers to prepare visible light active $Bi_2WO_6/Ta_3N_5$Z-scheme heterojunction photocatalyst. The catalyst within 120 min degrades 86.7% tetracycline hydrochloride. In presence of visible light irradiation, the catalyst follows type-II heterojunction, where CB and VB of $Bi_2WO_6$ are more positive than $Ta_3N_5$. As a result, photoexcited electrons of $Ta_3N_5$ drift to $Bi_2WO_6$, meanwhile holes from $Bi_2WO_6$ transfer to $Ta_3N_5$. This type of electron-hole transportation increases the lifetime of ROS that enhance catalytic activity for pollutant degradation [32].

### *3.3. Hybrid Organic–inorganic Perovskites*

The general formula of hybrid organic–inorganic perovskites is $ABX_3$ where A, B, X represent an organic cation, an inorganic metal and a halogen element respectively. Such types of hybride perovskites show much affectivity in photocatalytic application due to fast electron and hole mobility, high absorption coefficient, suitable bandgap, reduced rate of electron-hole recombination [33, 34]. This type of perovskite is also termed as revolutionized photovoltaics due to their 25.2% power conversion efficiency [35]. The perovskite show excellent properties for dye degradation, hydrogen evolution, $CO_2$ to CO, photo-polymerization reduction through photocatalytic pathway [35, 36].

Lead free methylammoniumiodobismuthate perovskite ($(CH_3NH_3)_3Bi_2I_9$) shows high degradation efficiency for RhB, MB, reactive blue under visible light irradiation. The presence of carbon atom in the catalyst play several role for good catalytic activity of the sample like it increases surface acidity, decrease electron-hole recombination rate, broaden visible light absorption capability. In the degradation mechanism, photo-generated holes follow one electron oxidation step for the production of hydroxyl radicals. These hydroxyl radicals are mainly responsible for the decomposition of the chromophoric dye structure to organic acid and alcohols [34]. Narrow band gap (2 eV) characteristics cesium bismuth iodide ($Cs_3Bi_2I_9$) has been anchored with UV100–$TiO_2$ nanoparticles to increase visible light absorption capacity [1]. Organic-inorganic hybrid bromide perovskite shows good photocatalytic activity in aqueous media by the formation of composite with MOF. Nanocomposite $MAPbBr_3$@ZIF-8 (MA represent methyl amine, ZIF-8 represent zeoliticimidazolate framework) show excellent stability in aqueous media and visible light activity for the decomposition of organic pollutants. In-situ hydroxyl radicals are formed from the composite materials and take an important role for the degradation of methyl orange under visible or sunlight irradiation [37]. Graphitic carbon nitride (GCN) and cesium lead halide perovskite ($CsPbBrCl_2$) based type-II heterojuntion catalyst degrade Eosin B under visible light irradiation. 30 mg GCN content GCN-$CsPbBrCl_2$ composite material show 94% Eosin B degradation efficiency in 120 min. The CB of $CsPbBrCl_2$ is more negative than GCN and VB of GCN is more positive than other. This type of position favours the separation of electron and hole for the creation of ROS at the surface of the composite material. The adsorbed dye molecule at the catalyst surface easily degrades to the non-toxic substance by the reaction with ROS. The corresponding chemical reactions are given below [36]:

$$CsPbBrCl_2 - GCN + h\upsilon \rightarrow e_{CB}^- + h_{VB}^+$$

$$e_{CB}^- + O_2 \rightarrow O_2^{\bullet -}$$

$$O_2 + 2e^- + 2H^+ \rightarrow H_2O_2$$

$$H_2O_2 + e^- \rightarrow HO^\bullet$$

$$h_{VB}^+ + Dye \rightarrow CO_2 + H_2O$$

$$HO^\bullet + Dye \rightarrow CO_2 + H_2O$$

$$O_2^{\bullet -} + Dye \rightarrow CO_2 + H_2O$$

Cesium lead bromide quantum dots ($CsPbBr_3$ QDs) show high photocatalytic activity for the degradation of methyl orange (MO) and tetracycline hydrochloride in ethanol under visible light irradiation. Here, in the pollutant degradation $O_2$ easily form $^\bullet O_2^-$ and take part in oxidizing reaction [38].

***Table 1.*** *Perovskite photocatalytic materials for wastewater treatment.*

| Catalyst | Pollutant | Degradation efficiency | Condition | References |
|---|---|---|---|---|
| $(CH_3NH_3)_3Bi_2I_9$ | RhB | 98% | Neutral pH, visible light irradiation, 3h | [34] |
| $LaNiO_3/TiO_2$ | MO | 100% | 150 min, 10 mg/L | [13] |
| | Ciprofloxacin | 54% | 210 min | |
| $ZnSn(OH)_6$ | MB | 88.4% | 100 min, natural sunlight, 5 mg/L pollutant | [21] |
| $CuSn(OH)_6$ | | 73.04% | | |
| $BaBiO_3$ | RhB | 83% | 240 min, natural pH, 450W Xe lamp, 5 mg/L pollutant | [22] |
| $LaFeO_3/TiO_2$ NTAs | MB | 69.7% | 120 min, natural pH, 500 W tungsten-halogen lamp, 10 mg $L^{-1}$ pollutant | [17] |
| BWO-OV/OCN | Tetracycline | 96.16% | 60 min, 300 W Xe lamp, 10 mg $L^{-1}$ pollutant | [31] |
| $SrTiO_3$(La, Cr) | Tetracycline | 83% | 90 min, 300 W Xe lamp, 20 mg $L^{-1}$ pollutant | [24] |
| Ti substituted $LaFeO_3$ | 4-chloro phenol | 100% | 120 min, UV-A light, neutral pH | [25] |
| GCN-$CsPbBrCl_2$ | Eosin B | 94% | 120 min, 500 W Xenon lamp, 20 mg catalyst in 40 ml of $10^{-5}$M pollutant | [36] |
| $CsPbBr_3$ QDs | MO | 70% | 30 min, 10 mg $L^{-1}$ pollutant | [38] |
| | Tetracycline | 76% | | |
| 2% Gd-doped $CoTiO_3$ | MB | 43.64% | 120 min, 300 W Xenon lamp, 0.04g photocatalyst in 100 ml 5ppm Methylene blue | [26] |
| 2% Gd-doped $CuTiO_3$ | | 74.19% | | |
| 2% Gd-doped $NiTiO_3$ | | 88.64% | | |
| $BiFeO_3$-$Bi_2S_3$ | MB | 97% | 18h, 20 mg photocatalyst in 10 ml 10 mg $L^{-1}$ pollutant | [27] |
| $SrTiO_3/MnFe_2O_4$ | Tetracycline | 100% | 20 min, 300 W microwave-200 W ultraviolet system, 22 mg/L pollutant | [28] |
| $Ba_{0.9}Ce_{0.1}Ti_{0.9}Mn_{0.1}O_3$ | Congo red | 91.95% | 60 min, natural solar light, natural pH, 0.025 mM pollutant | [29] |
| | Titan yellow | 82.45% | 120 min, natural solar light, natural pH, 0.025 mM pollutant | |

# 4. Active Species Trapping and ESR Study

In photocatalytic reaction, the identification of ROS is necessary to distinguish the path of reaction, improve degradation efficiency, involvement of several techniques for practical application [5]. The reactive oxygen species are generally superoxide anion radical, hydroxyl radical, hydrogen peroxide, singlet oxygen, electron, hole.

***Table 2.*** *List of scavengers for several ROS in photocatalytic mechanism study.*

| Reactive species | Scavenger | Pollutant | Catalyst | Reference |
|---|---|---|---|---|
| $^{\bullet}OH$ | Isopropanol | Tetracycline | $SrTiO_3$(La, Cr) | [24] |
| | | Tetracycline | $Bi_2WO_6/Ta_3N_5$ | [32] |
| | | MO | $MAPbBr_3$@ZIF-8 | [37] |
| | | Tetracycline | $SrTiO_3/MnFe_2O_4$ | [28] |
| | tert-butanol | Tetracycline | $CsPbBr_3$ QDs | [38] |
| | | MB | 2% Gd-doped $MTiO_3$ (M=Co, Cu, and Ni) | [26] |
| $^{\bullet}O_2^-$ | p-benzoquinone | MO | $MAPbBr_3$@ZIF-8 | [37] |
| | | Tetracycline | CsPbBr3 QDs | [38] |
| | | MB | 2% Gd-doped $MTiO_3$ (M=Co, Cu, and Ni) | [26] |
| | | Tetracycline | $SrTiO_3/MnFe_2O_4$ | [28] |
| e- | Silver nitrate | Tetracycline | $SrTiO_3$(La, Cr) | [24] |
| Hole (h+) | Methanol | Tetracycline | $SrTiO_3$(La, Cr) | [24] |
| | di-ammonium oxalate | MB | 2% Gd-doped $MTiO_3$ (M=Co, Cu, and Ni) | [26] |
| | EDTA-2K | MO | $MAPbBr_3$@ZIF-8 | [37] |
| | ethylenediaminetetraacetic acid | Tetracycline | CsPbBr3 QDs | [38] |
| | disodium ethylenediaminetetraacetic acid | Tetracycline | $SrTiO_3/MnFe_2O_4$ | [28] |

Jiang *et al*. has been used isopropanol, silver nitrate, and methanol for the identification of $^{\bullet}OH$, $e^-$, and hole respectively. They have done a control experiment under bubbling of $N_2$ gas to identify the effect of $^{\bullet}O_2^-$. In this study, $^{\bullet}O_2^-$ is taken an important role due to significant decrease of photocatalytic reaction rate by the time of control experiment [24]. In the photocatalytically degradation of MO by $MAPbBr_3$@ZIF-8, Mollik *et al*. have been used $AgNO_3$ (radical scavenger), EDTA-2K ($h^+$ scavenger), isopropanol ($^{\bullet}OH$), p-benzoquinone ($^{\bullet}O_2^-$ scavenger) to distinguish the reactive species [37]. $Bi_2WO_6/Ta_3N_5$ heterojunction exhibits a sharp decrease of degradation efficiency for tetracycline degradation in presence of isopropyl alcohol than benzoquinone and ammonium oxalate. The activity of hydroxyl radical is also established from the electron spin resonance (ESR) technique, where DMPO-$^{\bullet}OH$ signal is more contrast than DMPO-$^{\bullet}O_2^-$ [32]. Visible light mediated tetracycline degradation by $CsPbBr_3$ QDs shows that superoxide anion radicals take an important role than other ROS. The less influence of hydroxyl radical is due to the

standard reduction potential of $^{\bullet}OH$ /$OH^{-}$ (+1.99 eV) is more positive than VB potential of $CsPbBr_3$ QDs (+1.81 eV). In the other side, the standard redox potential of $O_2$/$^{\bullet}O_2^{-}$ (-0.33 eV) is less negative than CB potential (-0.45 eV) of $CsPbBr_3$ QDs [38]. In tetracycline degradation by $SrTiO_3$/$MnFe_2O_4$ microwave-ultraviolet system, trapping experiment shows that $^{\bullet}OH$ takes an important and major role. ESR technique is also supported the above ROS, as the high intensity 1:2:2:1 characteristics signal of DMPO-$^{\bullet}OH$ than 1:1:1:1 signal of DMPO-$^{\bullet}O_2^{-}$ [28].

# 5. Future Prospectus and Conclusion

Perovskite photocatalyst materials have great interest in photocatalytic application for wastewater treatment. A huge number of research has been done on doped and undoped perovskite material to enhance the photocatalytic property. The main aim to find a suitable photocatalyst, which is based on the reduction of bandgap energy, visible light activity, separation efficiency of electron-hole, easy generation of reactive oxygen species, recyclability of photocatalyst, low cost, easy operation, large industrial application, no secondary pollutant, and environmental friendly nature. Though some disadvantages are removed but a lot of work till pending for future like (i) rate of the reaction, (ii) recovery of the photocatalyst, (iii) practical large scale based work, (iv) design of photocatalytic reactor for speedy process, (v) involvement of natural solar light. The research also takes place on the basis of the surface/interface process at atomic level to understand the action of the photocatalyst surface.

The review is based on the activity of perovskite material for wastewater treatment under light irradiation. The progress of research shows involvement of different design strategies, variation of chemical formula, morphology engineering, heterojunction formation etc. The generation of ROS and their non-selective involvement in pollutant degradation prefer no secondary pollutant generation. Most of the studies have been done in laboratory scale with artificial solar light irradiation which does not give the real impact of future applicability.

# Acknowledgements

AD gratefully thanks Department of Chemistry, Balarampur College for the infrastructure facilities provided. The authors express their thankfulness to Dr. Bhaskar Biswas for his expensive inputs in the preparation of this review.

# References

[1] B.-M. Bresolin, N. O. Balayeva, L. I. Granone, R. Dillert, D. W. Bahnemann, M. Sillanpää, Anchoring lead-free halide Cs3Bi2I9 perovskite on UV100–$TiO_2$ for enhanced photocatalytic performance, Sol. Energy Mater. Sol. Cells. 204 (2020) 110214.

[2] J. Briffa, E. Sinagra, R. Blundell, Heavy metal pollution in the environment and their toxicological effects on humans, Heliyon. 6 (2020) e04691. https://doi.org/https://doi.org/10.1016/j.heliyon.2020.e04691.

[3] S. O. Ganiyu, C. A. Martínez-Huitle, M. A. Rodrigo, Renewable energies driven electrochemical wastewater/soil decontamination technologies: A critical review of fundamental concepts and applications, Appl. Catal. B Environ. (2020) 118857.

[4] V. S. Arutyunov, G. V Lisichkin, Energy resources of the 21st century: problems and forecasts. Can renewable energy sources replace fossil fuels?, Russ. Chem. Rev. 86 (2017) 777–804. https://doi.org/10.1070/rcr4723.

[5] Y. Nosaka, A. Y. Nosaka, Generation and Detection of Reactive Oxygen Species in Photocatalysis, Chem. Rev. 117 (2017) 11302–11336. https://doi.org/10.1021/acs.chemrev.7b00161.

[6] V. Dutta, S. Sharma, P. Raizada, R. Kumar, V. K. Thakur, V.-H. Nguyen, A. M. Asiri, A. A. P. Khan, P. Singh, Recent progress on bismuth-based Z-scheme semiconductor photocatalysts for energy and environmental applications, J. Environ. Chem. Eng. (2020) 104505.

[7] S. Huang, Y. Xu, Q. Liu, T. Zhou, Y. Zhao, L. Jing, H. Xu, H. Li, Enhancing reactive oxygen species generation and photocatalytic performance via adding oxygen reduction reaction catalysts into the photocatalysts, Appl. Catal. B Environ. 218 (2017) 174–185. https://doi.org/https://doi.org/10.1016/j.apcatb.2017.06.030.

[8] X. Zeng, T. Zhou, C. Leng, Z. Zang, M. Wang, W. Hu, X. Tang, S. Lu, L. Fang, M. Zhou, Performance improvement of perovskite solar cells by employing a CdSe quantum dot/PCBM composite as an electron transport layer, J. Mater. Chem. A. 5 (2017) 17499–17505. https://doi.org/10.1039/C7TA00203C.

[9] C. Cuhadar, S.-G. Kim, J.-M. Yang, J.-Y. Seo, D. Lee, N.-G. Park, All-Inorganic Bismuth Halide Perovskite-Like Materials A3Bi2I9 and A3Bi1.8Na0.2I8.6 (A=Rb and Cs) for Low-Voltage Switching Resistive Memory, ACS Appl. Mater. Interfaces. 10 (2018) 29741–29749. https://doi.org/10.1021/acsami.8b07103.

[10] J. Liang, F. Liu, M. Li, W. Liu, M. Tong, Facile synthesis of magnetic Fe3O4@BiOI@AgI for water decontamination with visible light irradiation: Different mechanisms for different organic pollutants degradation and bacterial disinfection, Water Res. 137 (2018) 120–129. https://doi.org/https://doi.org/10.1016/j.watres.2018.03.027.

[11] L. Lu, M. Lv, G. Liu, X. Xu, Photocatalytic hydrogen production over solid solutions between BiFeO3 and SrTiO3, Appl. Surf. Sci. 391 (2017) 535–541. https://doi.org/https://doi.org/10.1016/j.apsusc.2016.06.160.

[12] X. Sun, Y. Xie, F. Wu, H. Chen, M. Lv, S. Ni, G. Liu, X. Xu, Photocatalytic Hydrogen Production over Chromium Doped Layered Perovskite Sr2TiO4, Inorg. Chem. 54 (2015) 7445–7453. https://doi.org/10.1021/acs.inorgchem.5b01042.

[13] C. Chen, J. Zhou, J. Geng, R. Bao, Z. Wang, J. Xia, H. Li, Perovskite LaNiO3/$TiO_2$ step-scheme heterojunction with enhanced photocatalytic activity, Appl. Surf. Sci. 503 (2020) 144287.

[14] A. Kumar, A. Kumar, V. Krishnan, Perovskite Oxide Based Materials for Energy and Environment-Oriented Photocatalysis, ACS Catal. 10 (2020) 10253–10315.

[15] R. L. Withers, L. Bourgeois, A. Snashall, Y. Liu, L. Norén, C. Dwyer, J. Etheridge, Chessboard/Diamond Nanostructures and the A-site Deficient, Li1/2–3x Nd1/2+xTiO3, Defect Perovskite Solid Solution, Chem. Mater. 25 (2013) 190–201. https://doi.org/10.1021/cm303239d.

[16] S.-M. Lam, J.-C. Sin, A. R. Mohamed, A newly emerging visible light-responsive BiFeO3 perovskite for photocatalytic applications: A mini review, Mater. Res. Bull. 90 (2017) 15–30. https://doi.org/https://doi.org/10.1016/j.materresbull.2016.12.052.

[17] C. Gong, Z. Zhang, S. Lin, Z. Wu, L. Sun, C. Ye, Y. Hu, C. Lin, Electrochemical synthesis of perovskite LaFeO3 nanoparticle-modified $TiO_2$ nanotube arrays for enhanced visible-light photocatalytic activity, New J. Chem. 43 (2019) 16506–16514. https://doi.org/10.1039/C9NJ03908B.

[18] N. Yahya, A. M. Nasir, N. A. Daub, F. Aziz, A. Aizat, J. Jaafar, W. J. Lau, N. Yusof, W. N. W. Salleh, A. F. Ismail, Visible light–driven perovskite-based photocatalyst for wastewater treatment, in: Handb. Smart Photocatalytic Mater., Elsevier, 2020: pp. 265–302.

[19] C. Karthikeyan, P. Arunachalam, K. Ramachandran, A. M. Al-Mayouf, S. Karuppuchamy, Recent advances in semiconductor metal oxides with enhanced methods for solar photocatalytic applications, J. Alloys Compd. 828 (2020) 154281.

[20] A. Ajmal, I. Majeed, R. N. Malik, H. Idriss, M. A. Nadeem, Principles and mechanisms of photocatalytic dye degradation on $TiO_2$ based photocatalysts: a comparative overview, RSC Adv. 4 (2014) 37003–37026. https://doi.org/10.1039/C4RA06658H.

[21] S. Dong, L. Cui, Y. Zhao, Y. Wu, L. Xia, X. Su, C. Zhang, D. Wang, W. Guo, J. Sun, Crystal structure and photocatalytic properties of perovskite MSn(OH)6 (M=Cu and Zn) composites with d10-d10 configuration, Appl. Surf. Sci. 463 (2019) 659–667. https://doi.org/https://doi.org/10.1016/j.apsusc.2018.09.006.

[22] A. M. Huerta-Flores, D. Sánchez-Martínez, M. del Rocío Hernández-Romero, M. E. Zarazúa-Morín, L. M. Torres-Martínez, Visible-light-driven BaBiO3 perovskite photocatalysts: Effect of physicochemical properties on the photoactivity towards water splitting and the removal of rhodamine B from aqueous systems, J. Photochem. Photobiol. A Chem. 368 (2019) 70–77. https://doi.org/https://doi.org/10.1016/j.jphotochem.2018.09.025.

[23] P. Mehdizadeh, O. Amiri, S. Rashki, M. Salavati-Niasari, M. Salimian, L. K. Foong, Effective removal of organic pollution by using sonochemical prepared LaFeO3 perovskite under visible light, Ultrason. Sonochem. 61 (2020) 104848.

[24] J. Jiang, Y. Jia, Y. Wang, R. Chong, L. Xu, X. Liu, Insight into efficient photocatalytic elimination of tetracycline over $SrTiO_3$(La, Cr) under visible-light irradiation: The relationship of doping and performance, Appl. Surf. Sci. 486 (2019) 93–101. https://doi.org/https://doi.org/10.1016/j.apsusc.2019.04.261.

[25] P. Garcia-Muñoz, C. Lefevre, D. Robert, N. Keller, Ti-substituted LaFeO3 perovskite as photoassisted CWPO catalyst for water treatment, Appl. Catal. B Environ. 248 (2019) 120–128. https://doi.org/https://doi.org/10.1016/j.apcatb.2019.02.030.

[26] S. Safari, S. M. Seyed Ahmadian, A. R. Amani-Ghadim, Visible light photocatalytic activity enhancing of MTiO3 perovskites by M cation (M=Co, Cu, and Ni) substitution and Gadolinium doping, J. Photochem. Photobiol. A Chem. 394 (2020) 112461. https://doi.org/https://doi.org/10.1016/j.jphotochem.2020.112461.

[27] Y. Subramanian, B. Mishra, S. Mandal, R. Gubendiran, Y. S. Chaudhary, Design of heterostructured perovskites for enhanced photocatalytic activity: Insight into their charge carrier dynamics, Mater. Today Proc. (2020).

[28] X. Wang, L. Jiang, K. Li, J. Wang, D. Fang, Y. Zhang, D. Tian, Z. Zhang, D. D. Dionysiou, Fabrication of novel Z-scheme SrTiO3/MnFe2O4 system with double-response activity for simultaneous microwave-induced and photocatalytic degradation of tetracycline and mechanism insight, Chem. Eng. J. 400 (2020) 125981.

[29] M. K. Adak, D. Mondal, S. Mondal, S. Kar, S. J. Mahato, U. Mahato, U. R. Gorai, U. K. Ghorai, D. Dhak, Ferroelectric and photocatalytic behavior of Mn-and Ce-doped BaTiO3 nanoceramics prepared by chemical route, Mater. Sci. Eng. B Solid-State Mater. Adv. Technol. 262 (2020) 114800. https://doi.org/https://doi.org/10.1016/j.mseb.2020.114800.

[30] Z. Hua, X. Zhang, X. Bai, L. Lv, Z. Ye, X. Huang, Nitrogen-doped perovskite-type La2Ti2O7 decorated on graphene composites exhibiting efficient photocatalytic activity toward bisphenol A in water, J. Colloid Interface Sci. 450 (2015) 45–53. https://doi.org/https://doi.org/10.1016/j.jcis.2015.02.061.

[31] X. Huo, Y. Yang, Q. Niu, Y. Zhu, G. Zeng, C. Lai, H. Yi, M. Li, Z. An, D. Huang, Y. Fu, B. Li, L. Li, M. Zhang, A direct Z-scheme oxygen vacant BWO/oxygen-enriched graphitic carbon nitride polymer heterojunction with enhanced photocatalytic activity, Chem. Eng. J. 403 (2021) 126363. https://doi.org/https://doi.org/10.1016/j.cej.2020.126363.

[32] S. Li, J. Chen, S. Hu, H. Wang, W. Jiang, X. Chen, Facile construction of novel $Bi_2WO_6/Ta_3N_5$ Z-scheme heterojunction nanofibers for efficient degradation of harmful pharmaceutical pollutants, Chem. Eng. J. 402 (2020) 126165. https://doi.org/https://doi.org/10.1016/j.cej.2020.126165.

[33] Q. Chen, N. De Marco, Y. (Michael) Yang, T.-B. Song, C.-C. Chen, H. Zhao, Z. Hong, H. Zhou, Y. Yang, Under the spotlight: The organic–inorganic hybrid halide perovskite for optoelectronic applications, Nano Today. 10 (2015) 355–396. https://doi.org/https://doi.org/10.1016/j.nantod.2015.04.009.

[34] B.-M. Bresolin, S. Ben Hammouda, M. Sillanpää, Methylammonium iodo bismuthate perovskite (CH3NH3)3Bi2I9 as new effective visible light-responsive photocatalyst for degradation of environment pollutants, J. Photochem. Photobiol. A Chem. 376 (2019) 116–126. https://doi.org/https://doi.org/10.1016/j.jphotochem.2019.03.009.

[35] Y. Dong, K. Li, W. Luo, C. Zhu, H. Guan, H. Wang, L. Wang, K. Deng, H. Zhou, H. Xie, Y. Bai, Y. Li, Q. Chen, The Role of Surface Termination in Halide Perovskites for Efficient Photocatalytic Synthesis, Angew. Chemie Int. Ed. 59 (2020) 12931–12937. https://doi.org/https://doi.org/10.1002/anie.202002939.

[36] T. Paul, D. Das, B. K. Das, S. Sarkar, S. Maiti, K. K. Chattopadhyay, CsPbBrCl2/g-C3N4 type II heterojunction as efficient visible range photocatalyst, J. Hazard. Mater. 380 (2019) 120855. https://doi.org/https://doi.org/10.1016/j.jhazmat.2019.120855.

[37] S. Mollick, T. N. Mandal, A. Jana, S. Fajal, A. V Desai, S. K. Ghosh, Ultrastable Luminescent Hybrid Bromide Perovskite@MOF Nanocomposites for the Degradation of Organic Pollutants in Water, ACS Appl. Nano Mater. 2 (2019) 1333–1340. https://doi.org/10.1021/acsanm.8b02214.

[38] X. Qian, Z. Chen, X. Yang, W. Zhao, C. Liu, T. Sun, D. Zhou, Q. Yang, G. Wei, M. Fan, Perovskite cesium lead bromide quantum dots: A new efficient photocatalyst for degrading antibiotic residues in organic system, J. Clean. Prod. 249 (2020) 119335. https://doi.org/https://doi.org/10.1016/j.jclepro.2019.119335.